BER performance of multiwavelength optical cross-connected networks with deflection routing

G.A. Castañón
O.K. Tonguz
A. Bononi

Indexing terms: Network routing, Optical crosstalk, Optical interconnections, Bit error rate

Abstract: The transmission performance of regular two-connected multihop transparent optical networks in uniform traffic under hot-potato, single-buffer deflection routing schemes is presented. Manhattan Street Network (MS) and ShuffleNet (SN) are compared in terms of bit error rate (BER) and packet error rate (PER) both analytically and by simulation. The authors implement a novel strategy of analysis, in which the transmission performance evaluation is linked to the traffic randomness of the networks. Amplifier spontaneous emission (ASE) noise, and device-induced crosstalk severely limit the characteristics of the network, such as propagation distance, sustainable traffic and bit rate. The results indicate that under the same load the BER performance of single-buffer deflection routing is worse than hot-potato. However, at BER = 10^{-9} single-buffer has a higher throughput than hot-potato. It is shown that the feasibility of deflection routing in transparent networks with MS and SN topologies heavily depends on the power coupling coefficient of the routing space switch used in each node.

1 Introduction

Transparent cross-connected optical networks with deflection routing have recently become the focus of much research [1–6]. The idea behind transparent networks is to modulate a lightwave carrier with data packets and let these optical packets travel from source to destination through a sequence of intermediate nodes without conversion to electronic form. Cross-connected topologies achieve higher throughput than linear topologies like buses and rings. If buffers are not available, the packets can be temporarily deflected to an undesired link. Thus, deflection routing allows use of fibre links as optical buffers [1–5]. However, the accumulation of weak noises such as the amplifier spontaneous emission (ASE) noise and the crosstalk introduced by the 2 × 2 space switches and by the wavelength demultiplexers/multiplexers (DEMUX/MUX) in the nodes causes a significant performance degradation in transparent networks.

The traffic performance of multihop packet-switching networks such as Manhattan Street Network (MS) [1] and ShuffleNet (SN) [3] have been studied extensively (see, for example [1–5]). However, relatively few studies consider the bit error rate (BER) performance of these networks ([6, 7]). In [6] ultrafast soliton communication is used to evaluate the BER and packet error rate (PER) in multihop networks with deflection routing, but the impact of crosstalk is not considered. In [7] the BER analysis appearing in [8] and [9] is extended using a semianalytical simulation method for estimating the effect of the interference (intersymbol interference, crosstalk) noises on the BER performance of a circuit switching network. However, the impact of traffic randomness is not considered in the analysis.

This paper presents the first complete BER and PER analysis based on the traffic randomness of multihop packet-switched transparent multiwavelength networks. It is shown that the BER performance strongly depends on the traffic load of the network and the transmission power. We present the limit of operation based on a uniform traffic scenario. The main impairments considered in the analysis are intraband crosstalk and ASE noise.

2 Node structure

The node is composed of a stack of submodules, one per wavelength. The wavelengths from the input fibres are spatially demultiplexed and sent to the appropriate submodule for add/drop operations and switching. Packets from the submodules are finally remultiplexed onto the output fibres. Fig. 1 shows a block diagram of the submodule described in [6].

With hot-potato routing the main switch is a simple crossbar switch. The scheme for a single-buffer memory is also shown in Fig. 1. A deflection occurs in the single-buffer scheme when three conflicting packets with the same output preference are present, two at the input links of the main switch and one in the buffer. The addition of more optical buffers reduces deflections but introduces more power losses and crosstalk. It will be shown that the presence of a single buffer can significantly degrade the transmission performance.

IEE Proceedings online no. 19971089

Paper first received 30th June and in revised form 20th December 1996

G.A. Castañón and O.K. Tonguz are with the Photonics Research Laboratory, Department of Electrical and Computer Engineering, State University of New York at Buffalo, Buffalo, NY 14260, USA

A. Bononi is with the Dipartimento di Ingegneria dell'Informazione, Università di Parma, I-43100 Parma, Italy

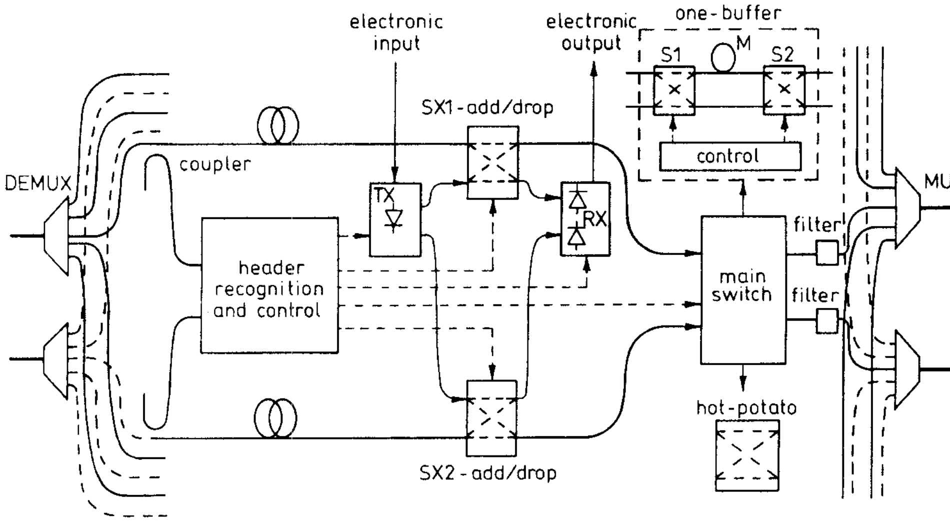

Fig. 1 *Node block diagram, hot-potato switch and one-buffer switch*
M is the memory, S1 and S2 are exchange-bypass switches

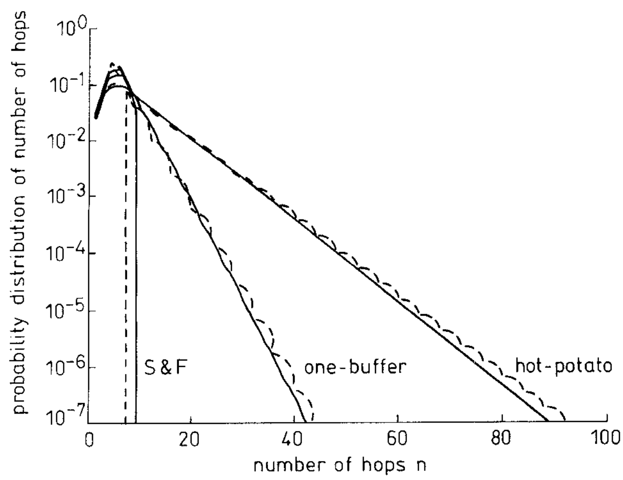

Fig. 2 *Probability distribution of number of hops against n*
——— MS64
– – – SN64

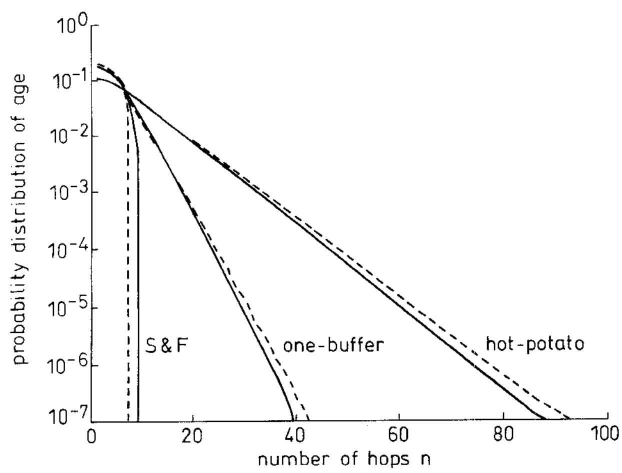

Fig. 3 *Probability distribution of the age against number of hops n*
——— MS64
– – – SN64

2.1 Traffic parameters

There are four parameters that determine the transmission performance [10]:

(*a*) Average number of hops H that packets experience before absorption. The probability of packet absorption a is related to H as: $a = 1/H$ [5]

(*b*) The probability mass function (pmf) of the number of hops taken by a typical packet before absorption, shown in Fig. 2 [5]

(*c*) The pmf of the age of packets, i.e. the number of hops experienced by a typical packet when it visits a generic node. This is depicted in Fig. 3 and an analytical method to derive it is presented in the Appendix. Such curves are important when the amplifier gain is not equal to the interamplifier loss, since packets have power variations depending directly on their age. Fig. 4 shows the average age A and Fig. 5 [5] shows H versus the probability of packet generation g

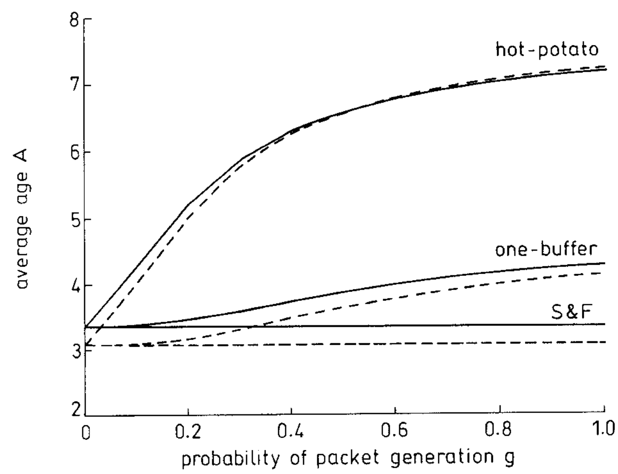

Fig. 4 *Average age A against packet generation g*
——— MS64
– – – SN64

(*d*) The link utilisation u is the probability of finding a packet at the input links of a node at each slot. When each submodule has two receivers and one transmitter, the link utilisation is [5]

$$u = \frac{\sqrt{a^2 + g^2(1-a)^2} - a}{g(1-a)^2} \quad (1)$$

3 Device-induced optical crosstalk

The crosstalk generated in a 2 × 2 space switch is due to incomplete switching. A fraction $1 - \alpha$ of the signal power exits from the desired port, while a fraction α leaks from the undesired port (see Fig. 1). If two signals at the same wavelength are present at the inputs, intraband crosstalk is generated.

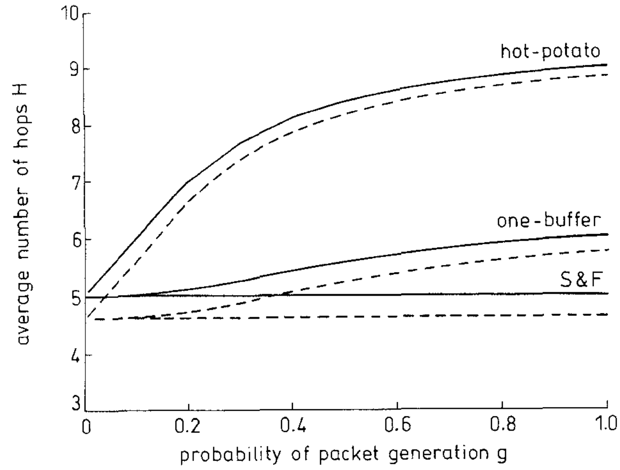

Fig. 5 *Average number of hops against packet generation g*
—— MS64
- - - SN64

A wavelength DEMUX behaves like a prism that fans out the light from the input fibre into distinct colour (wavelength) beams which are coupled to distinct outputs. The crosstalk in the DEMUX is (Fig. 1) due to residues of light from neighbouring colours on each output. This interband crosstalk becomes intraband crosstalk at the multiplexer (MUX) when colours are merged again on the output fibre [8]. The interband crosstalk can be reduced by placing narrowband optical filters before multiplexing. The amount of suppression of the interband components will depend on the transfer function $T(\Delta\lambda)$ of the filters.

4 Signal-to-noise ratio

The signal-to-noise ratio (SNR) at the output of a direct-detection receiver for on–off keying (OOK) modulation format can be expressed as [11]

$$SNR = \frac{RP_{sig}}{\sqrt{X(1)} + \sqrt{X(0)}} \qquad (2)$$

where $R = (\eta e/h\nu)$ is the photodetector responsivity (unit: ampere/watt), η is the quantum efficiency (unit: dimensionless), e is the electron's charge (unit: coulomb) and $h\nu$ is the energy of a photon (unit: joule). P_{sig} is the desired signal power during a mark, $X(1) = \sigma^2_{s\text{-}xt} + \sigma^2_{s\text{-}sp} + \sigma^2_{xt\text{-}xt} + \sigma^2_{xt\text{-}sp} + \sigma^2_{sp\text{-}sp}$ and $X(0) = \sigma^2_{xt\text{-}xt} + \sigma^2_{xt\text{-}sp} + \sigma^2_{sp\text{-}sp}$. The variance terms refer to the signal–crosstalk (s-xt), signal–ASE (s-sp), crosstalk–crosstalk (xt-xt), crosstalk–ASE (xt-sp) and ASE–ASE (sp-sp) beat terms, respectively. Contribution of shot and thermal noise were not included because they are negligible compared to the other beat terms.

Assuming that the polarisation and phase of the crosstalk signals are uniformly distributed random variables, and mark and space symbols are equally likely, such variances are given by [10]

$$\sigma^2_{s-xt} = R^2 \frac{P_{sig}P_{xt}}{2} \qquad (3)$$

$$\sigma^2_{xt-xt} = R^2(N-1)\frac{P^2_{xt}}{8N} \qquad (4)$$

$$\sigma^2_{xt-sp} = 2\frac{B_e}{B_o}R^2 P_{xt}P_{ase} \qquad (5)$$

where B_e is the electrical filter bandwidth, B_0 is the optical filter bandwidth, N is the number of crosstalk interferers ($N \geq 1$) and P_{xt} is the accumulated crosstalk power. P_{ase} is the accumulated amplifier noise. In the worst case, when one considers polarisation matching for all the beat interferers, the terms $\sigma^2_{xt\text{-}xt}$ and $\sigma^2_{s\text{-}xt}$ are scaled up by a factor of two. Equations for signal–spontaneous

$$\sigma^2_{s-sp} = \frac{4B_e}{B_o}R^2 P_{sig}P_{ase}$$

and spontaneous–spontaneous

$$\sigma^2_{sp-sp} = R^2\frac{B_e(2B_o - B_e)}{B^2_o}P^2_{ase}$$

beat terms are given in [11, 12].

5 Evaluation of crosstalk

5.1 Analysis

This Section will derive the necessary equations to compute the signal power, crosstalk and ASE noise, at any traffic load, of a test packet travelling in a cross-connected network. It is assumed that

(i) The bit times of all channels are aligned

(ii) All lasers transmit with the same power P_{TX}

(iii) The internode distance is constant.

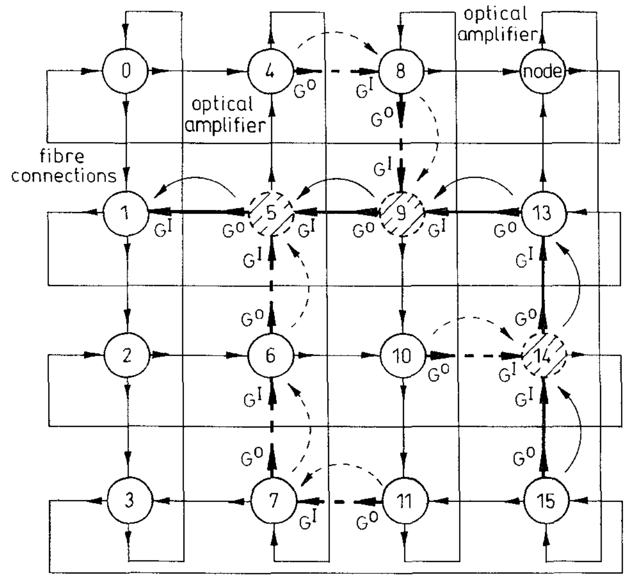

Fig. 6 *16-node Manhattan Street Network*
The bold line is the path of a test packet sent from node 15 to node 1, bold-dashed lines are the paths of the interference packets, narrow lines are generic cross-connections. Observe that the test packet experiences crosstalk in three of the nodes (the shadowed nodes 14, 9 and 5) and the interference packets have 1, 2 and 3 hops, respectively, as the arc-dashed arrows indicate. Optical amplifiers are located at the output and at the input of the node. Orientation of the amplifiers also indicate the communication direction. The architecture of each node is the same and is given in Fig. 1

An example of the scenario analysed is shown in Fig. 6. The bold line in Fig. 6 is the path of a test packet sent from node 15 to node 1, bold-dashed lines are the paths of the interference packets, and narrow lines are generic cross-connections. In this paper only powers that interfere in a direct way with a test packet are considered because the power coupling coefficient $\alpha << 1$. The total power ($P_{RE,i}$) of the test packet is

$$P_{RE,i} = (P_{sig,i} + P_{xt,i} + P_{ASE,i} + P^{ASE}_{xt,i})G_{RE} + P_{ASE,RE} \qquad i = 1, 2, \ldots \qquad (6)$$

where the subscript i represents the number of hops. It can be observed from Fig. 1 that a hop starts and ends after the ADD/DROP switch. G_{RE} is the receiver gain and $P_{ASE,RE}$ is the ASE noise produced by the receiver's amplifier, if a preamplified direct-detection receiver is used. The signal power is

$$P_{sig,i} = P_{TX} L^S L_\pi^i \quad i = 1, 2, \ldots \tag{7}$$

$L_\pi = L^{R1} L^{R2} L^M G^O L^F G^I L^D L^C L^S$ where the right-hand side terms are the loss of the first router switch (see Fig. 1), loss of the second router switch (for the case of single buffer), MUX loss, gain of the output amplifier (see Fig. 6), fibre loss, gain of the input amplifier, DEMUX loss, coupling loss and ADD/DROP switch loss, respectively. In case of hot-potato $L^{R2} = 1$. If only the output amplifier (input amplifier) is present, then $G^I = 1$ ($G^O = 1$).

$$P_{xt,i} = \left[\left\{(P_{xt,i-1} + \Upsilon_{sw1}) L^{R1} + \Upsilon_{sw2}\right\} L^{R2} L^M + \xi_{D-M}\right] \times G^O L^F G^I L^D L^C L^S \quad i = 1, 2, \ldots \tag{8}$$

where $P_{xt,0} = 0$. Eqn. 8 represents the accumulation of crosstalk noise. It considers the switch intraband crosstalk and the DEMUX/MUX intraband crosstalk. The first switch crosstalk term is

$$\Upsilon_{sw1} = \begin{cases} u(1-a) P_{xt,A} & \text{if } i = 1 \\ u(1-a) P_{xt,A} + [uag + (1-u)g] P_{XT} L^S \alpha & \text{otherwise} \end{cases} \tag{9}$$

When $i = 1$ the crosstalk statistic represents the probability of having a packet at the input of the main switch block (see Fig. 1) given that a test packet was generated by a node. This event occurs if a packet is present and not absorbed. When $i > 1$ we add the crosstalk probability of a new generated packet present at the input of the main switch. Hence, $uag + (1 - u)g$ represents the probability of having a packet present, the packet absorbed and a new packet generated, or the input link is empty and a new packet is generated. In eqn. 9 the crosstalk produced by the ADD/DROP switch has been neglected because the probability of adding and dropping a packet at the same time and by the same switch is negligible.

Now, when use is made of a single-buffer optical memory proposed in [5], the second switch crosstalk term is

$$\Upsilon_{sw2} = u P_{xt,A} L^{R1} \tag{10}$$

where the probability of memory being full can be approximated as $p_m \simeq u$. Also, the probability of packet crosstalk at the second switch can be approximated as p_m.

The DEMUX-MUX intraband crosstalk is

$$\xi_{D-M} = \begin{cases} \frac{u^2(1-a)}{2} \aleph (P_{sig,A} + P_{xt,A}) \times \Psi_D T(\Delta\lambda) L^{R1} L^{R2} L^M & \text{if } i = 1 \\ (1+u) \frac{u(1-a)}{2} \aleph (P_{sig,A} + P_{xt,A}) \times \Psi_D T(\Delta\lambda) L^{R1} L^{R2} L^M & \text{otherwise} \end{cases} \tag{11}$$

where $u(1 - a)/2$ is the probability of having an adjacent packet at the adjacent channel, such that it is not absorbed, and it is routed with the test packet with probability 0.5. Also $u^2(1 - a)/2$ is the probability of having a packet of the same wavelength, which is equal to u, at the second fibre multiplied by $u(1 - a)/2$. In eqn. 11 it is assumed that in the 'empty' slots the ADD/DROP switch is always in drop position to drain the noises from the network. In eqn. 11 the adjacent channel interband crosstalk produced by the demultiplexer is represented by Ψ_D The factor $\mathcal{N}$ can take values of 2 or 1 depending on the number of physical adjacent channels.

The ASE ($P_{ASE,i}$) noise is the one produced by the chain of optical amplifiers and ASE crosstalk noise of the interference packets ($P_{xt,i}^{ASE}$). Hence,

$$P_{ASE,i} = (P_{ASE,i-1} L_\beta + P_{sp}^O L^F G^I + P_{sp}^I) L^D L^C L^S \quad i = 1, 2, \ldots \tag{12}$$

where $L_\beta = L^{R1} L^{R2} L^M G^O L^F G^I$, $P_{ASE,0} = 0$, $P_{sp}^{I/O} = n_{sp} m h\nu (G^{I/O} - 1) B$ [13], m is the effective number of modes, n_{sp} is the spontaneous emission factor, $h\nu$ is the energy of a photon and B is the optical bandwidth. If only the output amplifier is present $P_{sp}^I = 0$ and vice versa. The accumulation of ASE crosstalk noise can be derived following the logic of eqns. 8–11. The ASE crosstalk statistics are very similar to the signal crosstalk statistics. However, eqn. 12 is a good approximation to the total ASE noise power.

Eqn. 8 is a recursive transcendental equation for $P_{xt,A}$ and can be solved numerically using a first-order approximation $P_{xt,A} \cong \alpha P_{sig,A}/(1 - \alpha)$. However, this value of $P_{xt,A}$ is a good approximation in itself, whereby the contribution of DEMUX/MUX crosstalk is neglected.

5.2 Simulation analysis

In the simulations performed, crosstalk is modelled [10] according to the traffic parameters of the network; i.e. g, a, u probabilities, *pmf* of the age of the packets, architecture of the submodules and routing algorithm [2]. The signal, crosstalk and ASE noise powers are computed depending on the hop number. The power levels are affected by the respective network losses. A well known EDFA model [13] is used to compute the output powers according to the characteristics of a real optical amplifier. The BER is processed by a routine for the BER calculation depending on the signal, crosstalk and ASE noise powers.

6 Results

In deflection routing the BER is obtained by conditioning the BER(n) on the number of hops n taken by a typical packet as [6]

$$BER = \sum_{n=1}^{\infty} BER(n) P(n) \tag{13}$$

The hop distribution $P(n)$ (Fig. 2) depends on network topology, routing and load, while the conditional BER(n) depends on the traffic load and the optical characteristics of the network. Similarly PER $= \Sigma_{n=1}^{\infty} \{1 - [1 - BER(n)]^M\} P(n)$ [6] where M is the number of bits in the packet.

We analysed a network with four 2.5Gb/s channels in the range of 1550nm to 1556nm, with 2nm channel separation. DEMUX with adjacent signal interband crosstalk of –30dB, and 2 × 2 crossbar optical switch with α between –25dB and –35dB are assumed. Filters have a transfer function $T(\Delta\lambda) = -17$dB. We represent each amplifier by using the spectrally resolved numerical model of [13] with a forward pumping scheme. The absorption and gain parameters are the same as those of [14] (see fibre 2a in [14]) with a length of 20m and a pump power of 50mW. Thus, it is assumed that the EDFAs are operating in the saturated regime. A bandwidth of 125GHz is used to resolve the effect of ASE spectrum. The optical filter at the receiver has a 0.2nm bandwidth and the electric filter has a 2.5GHz bandwidth. We assumed a fibre with dispersion coefficient D_c = 1 ps/km-nm, a loss coefficient of 0.2dB/km, an internode distance of 15km, a total node loss of 12.5dB for hot-potato and 15.5dB for single-buffer node architectures. The loss per single 2 × 2 switch is 3dB. Two cases of the optical amplifier locations are analysed: output amplifier location (A) and input amplifier location (B).

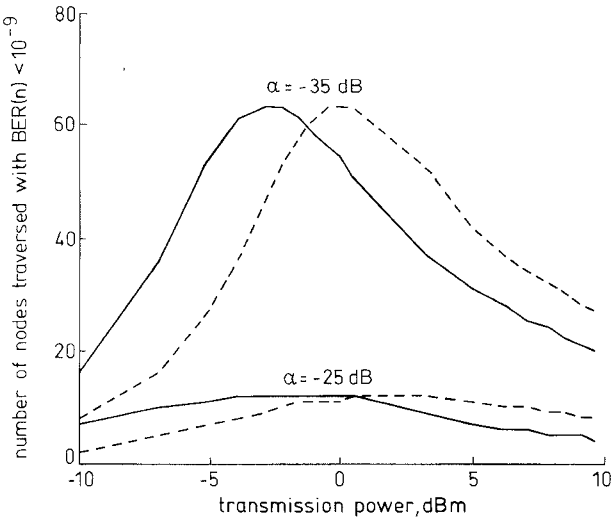

Fig. 7 *Maximum number of nodes traversed by a packet with a conditional BER(n) < 10^{-9} versus input power at g = 1, λ = 1556 nm*
Hot-potato under SN topology
——— case A
– – – – case B

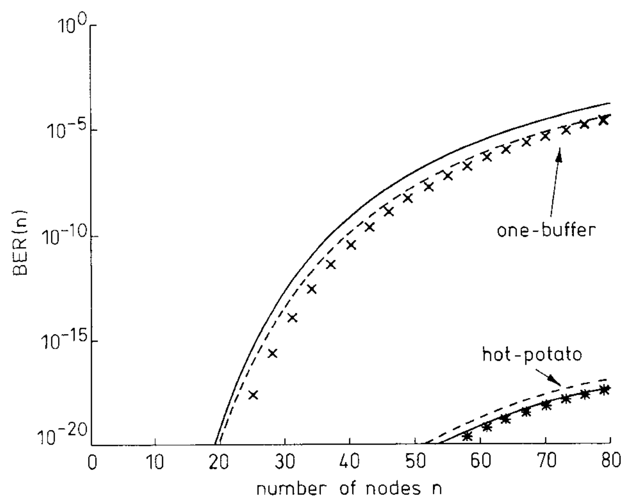

Fig. 8 *BER(n) against number of nodes for g = 0.1, α = –35 dB, λ = 1556 nm*
——— MS (simulation)
– – – SN (simulation)
* hot-potato SN (theory)
× one-buffer SN (theory)

We optimised each configuration based on the input power. Thus, Fig. 7 shows the maximum number of nodes traversed by a packet with a conditional BER(n) < 10^{-9} versus input power at g = 1 for the channel at 1556nm, the one with the worst gain. Results are shown for hot-potato under SN topology with α = –35dB and –25dB. Observe that the BER(n) performance is affected by the value of the power coupling coefficient α. For low input power the predominant beat noise is signal–ASE that increases with bit rate and for high input powers the signal–crosstalk limits the network, a noise that is bit-rate-independent. The reason that case A performs better than case B for low input power is that A keeps the signal power at a good level because it is amplified after the node. In the case of B the signal power is attenuated by the fibre span loss and then amplified, getting a lower power level with respect to case A and in this way affecting the BER(n). Since configuration A require less input power than B, we will only consider case A in the remainder of this paper.

Fig. 8 shows theoretical and simulation results for the conditional BER(n) versus number of nodes traversed by a packet when g = 0.1 for all the submodules of a network with 64 nodes. We used the Q(SNR) function approximation [15] to obtain the BER(n). Observe that SN and MS have a very similar BER(n) performance. The reason is that the link utilisation probability u and the average age A of the packets of both topologies are similar.

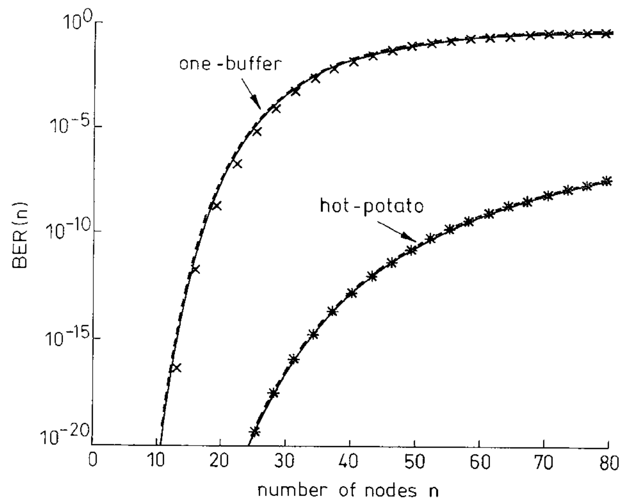

Fig. 9 *BER(n) against number of nodes for g = 1, α = –35 dB, λ = 1556 nm*
——— MS (simulation)
– – – SN (simulation)
* hot-potato SN (theory)
× one-buffer SN (theory)

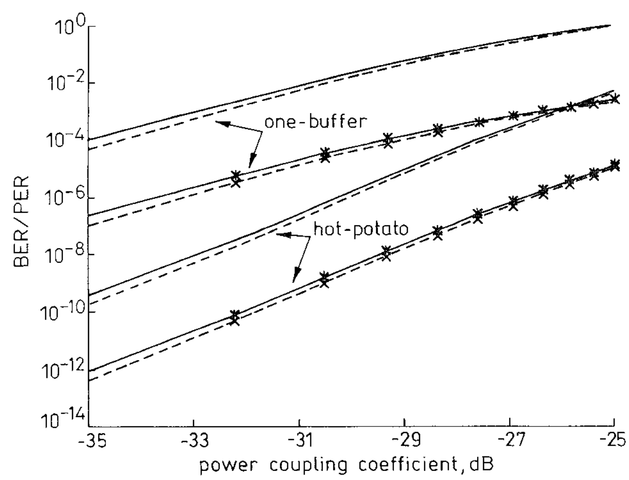

Fig. 10 *Bit error probability BER and packet error rate (PER) against power coupling coefficient α for g = 1*
– – – MS (PER)
——— SN (PER)
×– –× MS (BER)
—— SN (BER)

Fig. 9 shows results for the case when g = 1. Observe that the BER(n) degrades with full load. This is because there are more packets in the network and the crosstalk probability increases. The two main reasons why single-buffer has a worse BER(n) than hot-potato are: first, single-buffer has two optical switches to route the packets, therefore more intraband crosstalk; secondly ASE noise increases because the EDFAs gain increases (recall that the optical amplifiers are operating in the saturated mode) trying to compensate the loss introduced by the the addition of optical switches. Thus, the greater number of optical switches increase the amount of crosstalk and loss. Therefore, using more optical buffers to reduce deflection will deteriorate the BER(n) substantially.

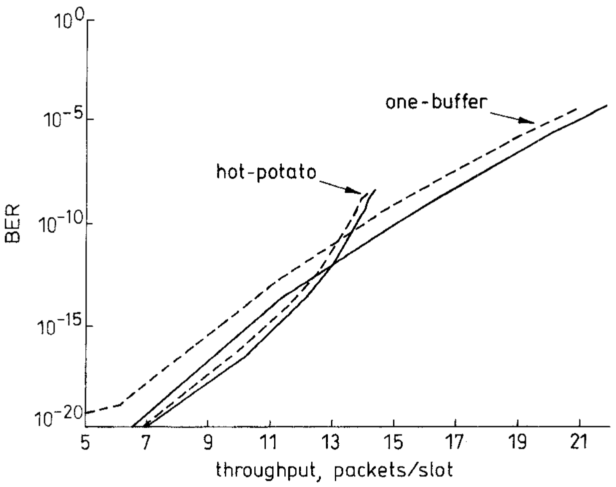

Fig. 11 *BER against throughput for networks with 64 nodes at α = −30 dB, λ = 1556 nm*
--- MS
—— SN

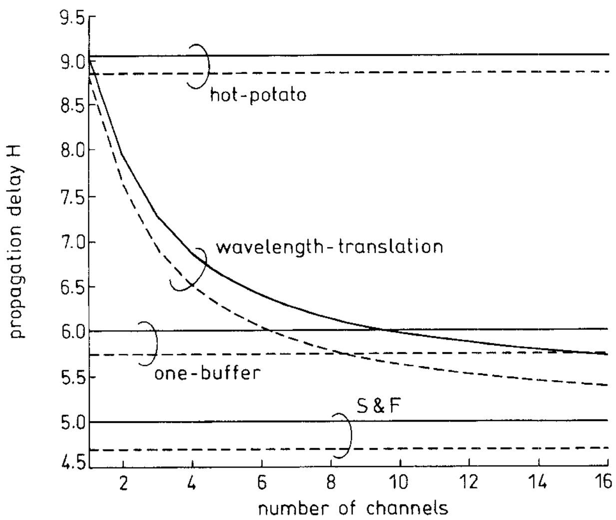

Fig. 12 *Simulation results of propagation delay H versus number of channels for hot-potato, single-buffer, store-and-forward (S&F) and wavelength translation at g = 1*
Results are for one of the channels. For the case of wavelength translation, packets on transit have translation priority over the new generated packets and wavelength used for the translation is chosen randomly among the available wavelengths.
—— MS64
--- SN64

Fig. 10 shows BER (using eqn. 13) and PER results versus α for a network of 64 nodes at g = 1. Observe that BER of single-buffer is always higher than 10^{-9} at full load. Otherwise, hot-potato depends on the power coupling coefficient. For $\alpha < -30.5$dB the BER $< 10^{-9}$ and vice versa. However, for a fair comparison of hot-potato and single-buffer, Fig. 11 shows BER versus throughput [5]. Observe that at BER = 10^{-9} single-buffer has a higher throughput than hot-potato owing to the superior teletraffic performance of single-buffer. Also, observe that under the same throughput SN has a better BER performance than MS as SN has less traffic congestion because the link load is lower and the packet absorption probability is higher.

There are certain ways to improve the performance of deflection routing. First, the teletraffic performance can be improved by a combination of deflection routing and wavelength translation (for a comprehensive analysis of wavelength translation in circuit-switching networks see for example [16]). In packet switching networks this has the feature of decreasing the probability of deflection, i.e. improving the throughput and propagation delay depending on the number of channels used in the network. Fig. 12 shows propagation delay H versus number of channels. Observe that propagation delay for hot-potato, single-buffer and store-and-forward (S&F [5, 10]) keeps constant because channels are independent of each other whereas propagation delay for wavelength translation routing improves with the number of channels. The reason is that packets in conflict have the possibility of being translated to an available slot with no conflict. Then the probability of deflection decreases and the propagation delay improves. Simulation results use uniform traffic conditions for each channel according to the method presented in [17] which we extended to wavelength translation. Further research is needed to address the physical implementation and design of wavelength translation scheme in packet switching networks. Also, the use of dilated switches could improve the transmission performance of deflection routing under certain conditions. Further research is needed to quantify the performance of MS and SN using dilated switches.

7 Conclusions

Crosstalk and ASE noise limit the propagation distance, traffic load and bit rate performance of the network. Our results indicate that under the same throughput SN has a better BER performance than MS. Results show that hot-potato deflection routing has a better BER performance than single-buffer at low throughput. However, at BER = 10^{-9} single-buffer has a higher throughput than hot-potato because single-buffer has less traffic congestion. If the bit rate increases the BER performance is worse than shown, but if it decreases the BER improves, making possible the operation of single-buffer at high throughput. However, if no special precautions (such as optimising the transmission power) are taken to reduce the intraband crosstalk, SN and MS networks will be limited to a few hops.

The feasibility of deflection routing in transparent networks will heavily depend on the isolation characteristics of the optical switching elements. The most crucial component is the routing space switch. A high power coupling coefficient α limits the operation of the network, while a low α will make its operation possible with good performance.

8 References

1 MAXEMCHUK, N.F.: 'The manhattan street network'. Proc. IEEE GLOBECOM '85, 1985, pp. 255–261
2 MAXEMCHUK, N.F.: 'Comparison of deflection and store-and-forward techniques in the manhattan street and shuffle-exchange networks'. Proc. IEEE INFOCOM '89, April 1989, pp. 800–809

3 ACAMPORA, A.S., KAROL, M.J., and HLUCHYJ, M.G.: 'Terabit lightwave networks: the multihop approach', *AT&T Tech. J.*, 1987, **66**, (6), pp. 21–34
4 CHLAMTAC, I., and FUMAGALLI, A.: 'An optical switch architecture for manhattan networks', *IEEE J. Sel. Areas Commun*, 1993, **11**, (4), pp. 550–559
5 FORGHIERI, F., BONONI, A., and PRUCNAL, P.: 'Analysis and comparison of hot-potato and single-buffer deflection routing in very high bit rate optical mesh networks', *IEEE Trans.*, 1995, **COM-43**, (1), pp. 88–98
6 BONONI, A., FORGHIERI, F., and PRUCNAL, P.: 'Design and channel constrain analysis of ultrafast multihop all-optical networks with deflection routing employing solitons', *IEEE J. Lightwave Technol.*, 1993, **11**, (12), pp. 2166–2176
7 ZHOU, J., CADEDDU, R., CASACCIA, E., CAVAZZONI, C., and O'MAHONY, M.J.: 'Crosstalk in multi-wavelength optical cross-connect networks', *IEEE J. Lightwave Technol.*, 1996, **14**, (14), pp. 1423–1435
8 ZHOU, J., O'MAHONY, M.J., and WALKER, S.D.: 'Analysis of optical crosstalk effects in multi-wavelength switched networks', *IEEE Photonics Technol. Lett.*, 1994, **6**, (2), pp. 302–305
9 GOLDSTEIN, E.L., ESKILDSEN, L., and ELREFAIE, A.: 'Performance implications of component crosstalk in transparent lightwave networks', *IEEE Photonics Technol. Lett.*, 1994, **6**, (5), pp. 657–660
10 CASTANON, G.A., TONGUZ, O.K., and BONONI, A.: 'Combined teletraffic/transmission performance of multiwavelength optical cross-connected networks using hybrid-store-and-forward', *IEEE J. Lightwave Technol.*, 1996, (submitted for publication)
11 RAMASWAMI, R., and HUMBLET, P.A.: 'Amplifier induced crosstalk in multichannel optical networks', *IEEE J. Lightwave Technol.*, 1990, **8**, (12), pp. 1882–1896
12 OLSSON, N.A.: 'Lightwave systems with optical amplifiers', *IEEE J. Lightwave Technol.*, 1989, **7**, (7), pp. 1071–1082
13 GILES, C.R., and DESUVIRE, E.: 'Modeling erbium-doped fibre amplifiers', *IEEE J. Lightwave Technol.*, 1991, **9**, (2), pp. 271–283
14 GILES, C.R., BURRUS, C., DIGIOVANNI, D., DUTTA, N., and RAYBON, G.: 'Characterization of erbium-doped fibre and application to modeling 980-nm and 1480-nm pumped amplifiers', *IEEE Photonics Technol. Lett.*, 1991, **3**, pp. 363–365
15 TONGUZ, O.K., and KAZOVSKY, L.G.: 'Theory of direct-detection lightwave receivers using optical amplifiers', *IEEE J. Lightwave Technol.*, 1991, **9**, (2), pp. 174–181
16 KOVACEVIC, M., and ACAMPORA, A.: 'On the benefits of wavelength translation in all-optical clear channel networks', *IEEE J. Sel. Areas Commun.*, 1996, **14**, (5), pp. 868–880
17 GREENBERG, A.G., and GOODMAN, J.B.: 'Sharp approximate models of deflection routing in mesh networks', *IEEE Trans. Commun.*, 1993, **41**, (1), pp. 210–223
18 ROSS, S.M.: 'Stochastic processes (Wiley & Sons, 1983, p.63)

9 Appendix

This Appendix will briefly recall the method used in [5] to get the hop distribution and average number of hops of a typical, or test packet generated uniformly at random at the network nodes and destined to a fixed target node. The method is extended to get the distribution of the hop-age of packets that cross a generic node, which is needed to assess the crosstalk levels added to the desired signal along its path.

The random walk of the test packet is modelled as a homogeneous absorbing Markov chain, whose states coincide with the network nodes. Let the nodes be numbered as 1, ..., N. Let node D be the destination (absorbing) node.

Let π_{ij} = Pr{test packet moves from node i to node j}. The transition probability matrix $\Pi = \{\pi_{ij}\}$ is completely specified once the deflection probability d, equal at each 'care' node for regular topologies, is given [5]. If $\mathbf{p}(0)$ is the initial (uniform) probability state vector, the state vector at the k-th hop is given by $\mathbf{p}(k) = \Pi^k\mathbf{p}(0)$. Each entry $p_i(k)$, $i = 1, ..., N$, represents the probability that the test packet visits node i at the k-th hop. The sum $\Sigma_{k=1}^{\infty} p_i(k) \triangleq E[V_i]$, $i = 1, ..., N$, where $E[\bullet]$ denotes the statistical expectation and $i \neq D$, represents the expected number of visits of transient node i by a test packet destined for node D excluding the injection step ($k = 0$). For the destination node, instead we have only one visit before absorption, i.e. $E[V_D] = 1$.

Hence $\hat{p}_i^{(D)}(k) \triangleq p_i(k)/E[V_i]$, $k = 1, 2, ..., i \neq D$, is the probability mass function (pmf) of the random variable $A_i^{(D)}$ = {hop-age of the test packet destined for node D, when it visits node i} since it is the probability that node i is visited at hop $k = 1, 2, ...$ conditioned on there being a visit of node i. The entry $p_D(k)$ = Pr{test packet is at the absorbing node D at time k} = Pr{absorption time $\leq k$} represents the cumulative distribution function (cdf) of the absorption time h, i.e. the number of hops taken by the test packet before absorption. From this, $\hat{p}_D^{(D)}(k) \triangleq p_D(k) - p_D(k-1)$ is the pmf of the hop-age of the test packet when it reaches the absorbing node, i.e. the hop distribution. Its mean value is the average number of hops $H^{(D)}$.

We are now interested in the pmf $p_A(k)$ of the hop-age of packets at a generic node i in uniform traffic. By conditioning on the destination D of the packet, this can be written as

$$p_A(k) = \sum_{D=1}^{N} \hat{p}_i^{(D)}(k) Pr\{D\} \tag{14}$$

where $Pr\{D\}$ is the probability that a packet destined for D visits node i, and can be estimated as the fraction of time packets to D are at node i, which according to the renewal theorem [18] is

$$Pr\{D\} = \frac{E[V_i^{(D)}]}{H^{(D)}} \quad D = 1, \ldots, N$$

If the network is regular, the entries $\{p_i^{(D)}(k), D = 1, ..., N\}$, except for a suitable relabelling of the nodes, are the same as the entries $\{p_i^{(D)}(k), i = 1, ..., N\}$, where the relabelling depends on the destination D. Also, the entries $\{E[V_i^{(D)}], D = 1, ..., N\}$, with the same relabelling, are equal to $\{E[V_i^{(D)}], i = 1, ..., N\}$, and thus $H^{(D)} = \Sigma_{i=1}^{N} E[V_i^{(D)}]$ does not depend on D.

Hence, after relabelling

$$\begin{aligned} p_A(k) &= \hat{p}_D^{(D)}(k)\frac{1}{H} + \sum_{\{ {i=1 \atop i\neq D} \}}^{N} \hat{p}_i^{(D)}(k)\frac{E[V_i^{(D)}]}{H} \\ &= \frac{1}{H}\left(p_D(k) - p_D(k-1) + \sum_{\{ {i=1 \atop i\neq D} \}}^{N} p_i(k) \right) \\ &= \frac{1 - p_D(k-1)}{H} \qquad k = 1, 2, 3, \ldots \end{aligned} \tag{15}$$

where we used the fact that $\Sigma_{i=1}^{N} p_i(k) = 1$. The last line of eqn. 15 is the operative formula for the hop-age pmf.